



AUTOMATIC MICROCRACK CHARACTERIZATION IN FRC-MATERIALS.

Henrik Stang
Department of Structural Engineering
Technical University of Denmark,
M.Sc. Ph.D., Research Engineer.

ABSTRACT

Microcracking is one of the key mechanisms governing the constitutive behaviour of Fibre Reinforced Cementitious materials.

Thus, quantitative characterization of microcracking patterns in FRC materials is an important tool in FRC material research. The microcracking patterns are usually too complicated to allow manual registration, thus computer aided registration is preferable.

The present paper describes an algorithm which makes automatic microcrack characterization possible without any interference from the operator, thus creating the possibility for obtaining unbiased data.

Finally the paper discusses some experimental observations in a specific FRC system.

Key-words: FRC-materials, Microcracking, Digital Image, Analysis, Stereology.

1. INTRODUCTION

The formation of cracks on the microscopic as well as the macroscopic level is the key to the understanding of the constitutive behaviour of cementitious materials. The introduction of a fibre reinforcement can drastically change the cracking behaviour. The changes are due to the fact that the fibers act as microcrack stabilizers (mainly through crack bridging), promoting the formation of stable microcracks rather than unstable microcracks.

As a consequence the efficiency of a given fibre reinforcement can be measured by its ability to produce distributed microcracking patterns rather than one localized crack.

Thus, with a means of characterizing microcracking patterns quantitatively it is possible to evaluate a given fibre/matrix system and - more important - to compare different fibres given the matrix.

If such evaluations are to be carried out it is of extreme importance that the quantitative measurements can be carried out in a reproducible way with as little human interference as possible. This requirement calls for a computer aided measurement system.

Fortunately a scientific and technical field has been developed over the past 10-20 years which aims specifically at transforming 2D image oriented information to digital information. This field is known as digital image processing and analysis.

In the following the application of basic tools from image processing and analysis in FRC microcrack characterization will be described, however, first a brief introduction to the basic concepts of image processing and analysis will be given.

2. PRINCIPLES OF DIGITAL IMAGE HANDLING

Several excellent introductions to digital image processing and analysis can be found in the literature today, /1/, /2/, /3/ and it is by no means the intention of this section to give an exhaustive review of this vast scientific field. However, a very brief introduction to the basic concepts will be given along with a description of the tools used in the present analysis.

A black and white digital image (which is the only kind of image considered here) can be thought of as an array of integers, with a - usually equal - number of rows and columns. A resolution of 512x512 is fairly standard. Low resolution images are usually 256x256 while 1024x1024 is usually considered high resolution images. Each element of the array is called a pixel and is usually represented by a number or grey value between 0 and 255, 0 corresponding to the lowest light intensity and 255 to the highest intensity.

Operations on the array corresponding to a digital image are usually divided into two main groups - those of image processing and those of image analysis. Image processing operations are basically concerned with the appearance of the image, while image analysis is concerned with deriving single numbers or sets of numbers quantifying properties of features shown in the image.

Image processing operators are typically filters or small arrays which operate on each of the pixels of the original image and determine a new value for the given pixel from the value of the original pixel and its surrounding pixels.

Consider eg. a so called 3x3 filter given by the 3x3 matrix

$$\begin{array}{ccc} f_{11} & f_{12} & f_{13} \\ f_{21} & f_{22} & f_{23} \\ f_{31} & f_{32} & f_{33} \end{array}$$

When placed somewhere on a digital image it tells us that the value of the center pixel should be replaced by a value which is computed by multiplying the pixel values with the corresponding elements of the filter matrix and then adding the results. Denoting the pixels covered by the filter by

$$\begin{array}{ccc} UL & UM & UR \\ ML & MM & MR \\ DL & DM & DR \end{array}$$

the new value of *MM* is given by

$$ULf_{11} + UMf_{12} + URf_{13} + MLf_{21} + MMf_{22} + MRf_{23} + DLf_{31} + DMf_{32} + DRf_{33}$$

The filter is now moved successively from pixel to pixel on the original image, thus producing the filtered image. A number of filters have been derived having sharpening or edge-enhancing effects, see eg. /1/, /2/, or /3/.

Another class of very important operations are contrast transformations. Such transformations are most easily described by means of transformation lines or curves in an x-y coordinate system which shows the 256 grey values of the original image on the x-axis and the 256 grey values of the new image on the y-axis. An example is shown in fig.1 where a transformation is shown which produces a negative image from the original one. A special case of the contrast transformations is the so called segmentation. This kind of transformation picks out pixels in a special intensity range and gives them all a special value while the rest of the pixels are turned off or set to zero intensity. Segmentation produces so called binary images which are images which contain only two kinds of pixels: pixels which are either turned off or on.

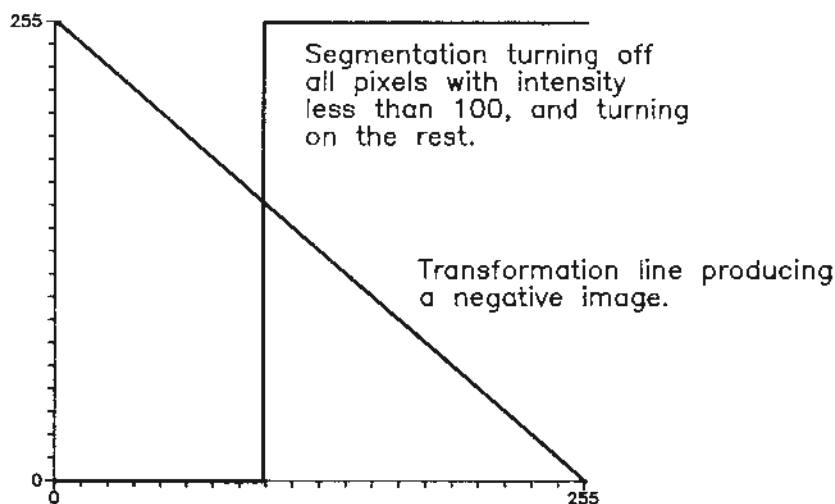


FIG. 1.

Fig.1. Contrast transformations shown by transformation lines. The values on the x-axis correspond to grey values of the original image while the y-axis gives the grey values of the transformed image.

A number of special kinds of operations can be performed on binary images, the most important being dilations, erosions, skeletonization and logical operations. Dilations turn on a single pixels layer around all the pixels already turned on, resulting in a swelling of all areas of turned on pixels. Erosion apply to all continuous areas of turned on pixels, removing a single layer from these areas. Skeletonization is a special kind of erosion reducing all continuous areas to tree-like structures of continuous lines. Especially very slender areas are reduced to single lines with a length corresponding to the largest dimension of the slender shape.

Logical operations are carried out by comparing binary images pixel by pixel. These operations are most easily explained by assigning the logical value 'true' to the pixels which are turned on, and 'false' to pixels turned off. All the conventional logical operations known from computer science (AND, OR, XOR, NOT) are then readily defined for binary images.

Finally the so called geometrical transformations should be mentioned. A geometrical transformation simply correspond to a movement of the pixel values a number of positions in the vertical and in the horizontal direction. Geometrical translations are defined for both ordinary and binary digital images.

3. THE EXPERIMENTAL PROCEDURE

The present investigation is concerned with microcrack initiation and growth in a special type of FRC materials namely cement pastes reinforced with aligned infinitely long polypropylene fibre rovings in volume concentrations in the range from 5 to 13%. The manufacturing and testing of these specimens are described in detail elsewhere /4/,/5/ thus only a brief outline will be given here.

The dog bone shaped tensile specimens are loaded in uniaxial tension with a prescribed strain rate of $1.67 \cdot 10^{-4}$ per second. Different test specimens are loaded to different axial strain levels, while their stress/strain response is recorded. Typical stress/ strain curves for a number of specimens with almost identical volume concentration but terminated at different strain levels are shown in fig.2.

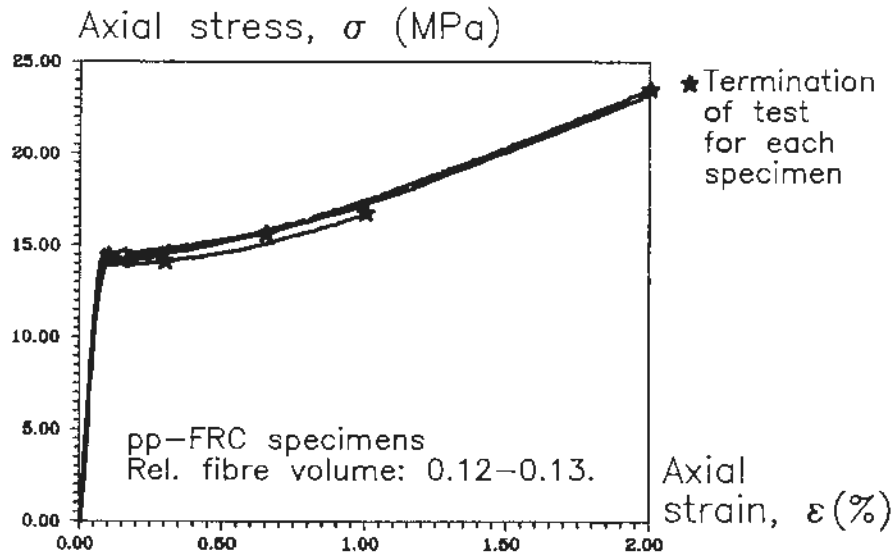


FIG. 2

Fig.2. Stress/ strain curves for polypropylene fibre reinforced cement paste. Six specimens with virtually the same fibre volume concentration is reported in this figure. The loading history for each specimen is terminated at a different strain level.

In order to record the microcracking pattern, steel blocks are glued to two sides of the specimens while the axial deformation is maintained by the testing machine, thus freezing the axial deformation. Hereafter the specimens are vacuum impregnated with fluorescent epoxy and thin sectioned. In this procedure the microcracks are filled with epoxy and are clearly visible in a conventional light microscope equipped for fluorescence analysis.

4. THE IMAGE PROCESSING AND ANALYSIS.

Consider a thin section taken from a test specimen with a given axial strain. Applying fluorescence analysis in the microscope the microcrack system becomes visible and an image is acquired using a high resolution video camera mounted on the microscope. This image is transferred to an image analysis system and digitized using the representation described above.

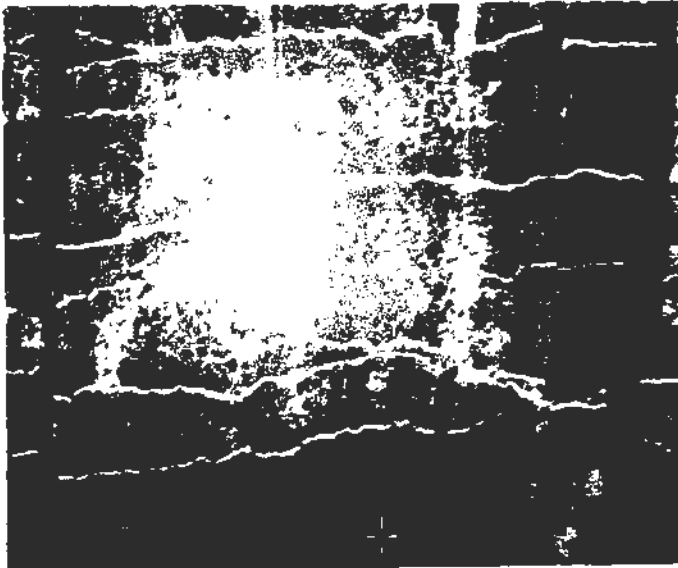


FIG.3

Fig.3. Observed microcracking pattern at 1% strain. The dark vertical line are the pp. fibres while the matrix cracks show up as bright horizontal lines.

The appearance of the original digitized image is shown in fig.3. A number of important observations can be made at this stage:

- Since fluorescence analysis is used in the analysis all light in the image comes from the fluorescent epoxy. If the specimen had been completely impermeable the thin section would appear black. The image thus reflects the permeable volume in the specimen at the time of vacuum impregnation.

- The cracks show up as bright horizontal lines. It is clear from fig.3. that the cracks are not the only permeable space in the specimens. Typically two families of voids and pores can be observed in the image: voids with a diameter considerably larger than the crack opening and voids or pores with a characteristic diameter of the same magnitude or smaller than the crack opening.

- Pixels which represent space completely filled with epoxy will have max. light intensity. If epoxy filled space only covers part of the area covered by the pixel, the intensity of the pixel will have a lower value. As a consequence of this pixels representing cracks will gradually loose light intensity as the crack tip is approached and the crack opening gets smaller than the pixel width .

It is clear from the observations made above that it is not possible to pick out crack pixels just by looking at the light intensity thus a segmentation alone cannot do the job. However, since manual registration is neither practical nor desirable the following algorithm was derived in order to deal with the problem outlined above.

- Enhance the original image by applying a standard 3x3 Laplacian filter, see /3/. This filter will produce a sharper image.

- Do a segmentation including all pixels with an intensity larger than a given value i . The value i is chosen so that all significant crack pixels are included. The corresponding binary image includes cracks as well as pores.

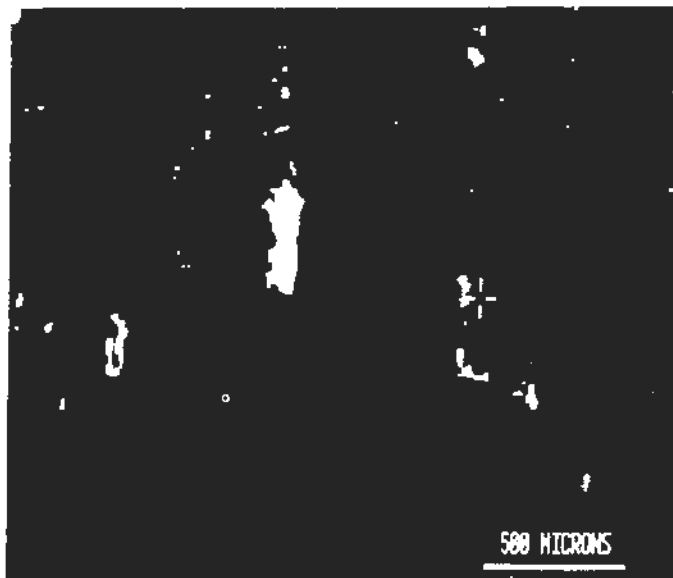


FIG.4

Fig.4. Binary image showing the larger pores only.

- Large voids are now removed automatically using the following concept. Imagine that the original binary is a transparency where the turned off pixels are non-transparent and assume that 3 copies of this transparency are also available. By translating the original and the three copies a distance ℓ upwards, downwards, to the left and to the right, the cracks will just have disappeared when ℓ correspond to half the largest crack opening.

The resulting image containing only the slightly reduced larger pores correspond exactly to the binary image obtained by translating the binary and three copies a distance ℓ and applying the logical 'AND' operator to the four images. The resulting binary image, see fig.4., is now dilated so that the pores regain their original size. Finally the larger pores are subtracted from the original binary by means of the logical 'NOT' and 'AND' operator. The cleaned binary is shown in fig.5.

- Smaller pores are now removed by subsequent erosion and dilation and finally the crack pattern is skeletonized. The final binary image is shown in fig.6. In this image all cracks detected are represented by single layer pixel lines.

When the image processing is finished the image analysis can be done. The purpose of the image analysis is to determine the total projected crack length on the horizontal (x) direction and the vertical (y) direction. In order to do that we need to know the pixel length in the two directions p_x and p_y . Next, each pixel is investigated. Due to the nature of the skeletonization process every turned on pixel will have a turned on neighbour above, and/or below and/or to the right and/or to the left, see fig.7. If the pixel only have a turned on neighbour to the left a projected crack length of $p_x/2$ in the x-direction is associated with it. If it has a turned on neighbour to the left and to the right then a projected crack length of p_x in the x-direction is associated with it and so on. Thus by investigating the turned on neighbours of each turned on pixel and doing a simple summation the total projected crack length ℓ_x and ℓ_y can be determined.

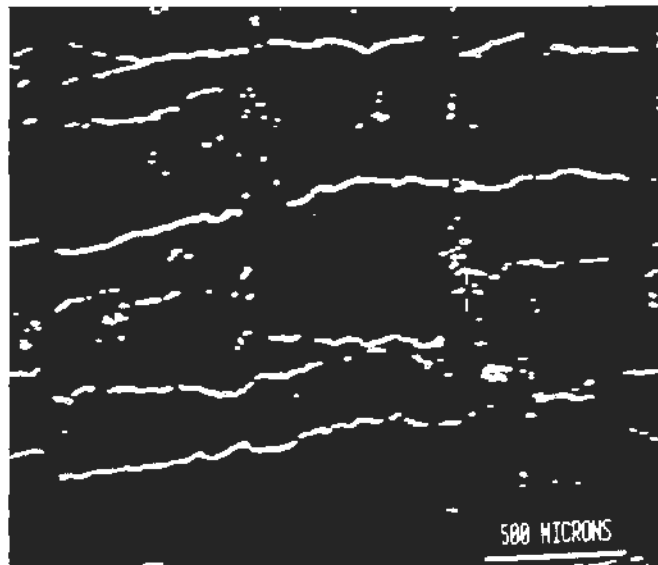


FIG.5

Fig.5. Binary image cleaned from larger pores.

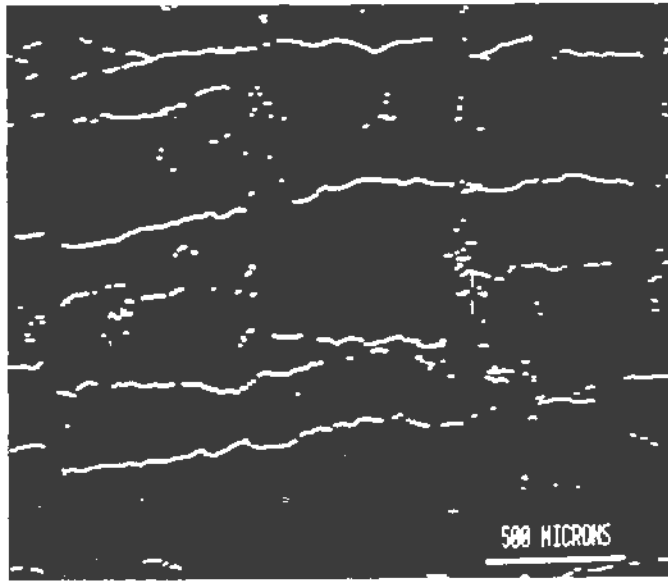


FIG.6

Fig.6. *Binary image showing only cracks as single pixel layer lines.*

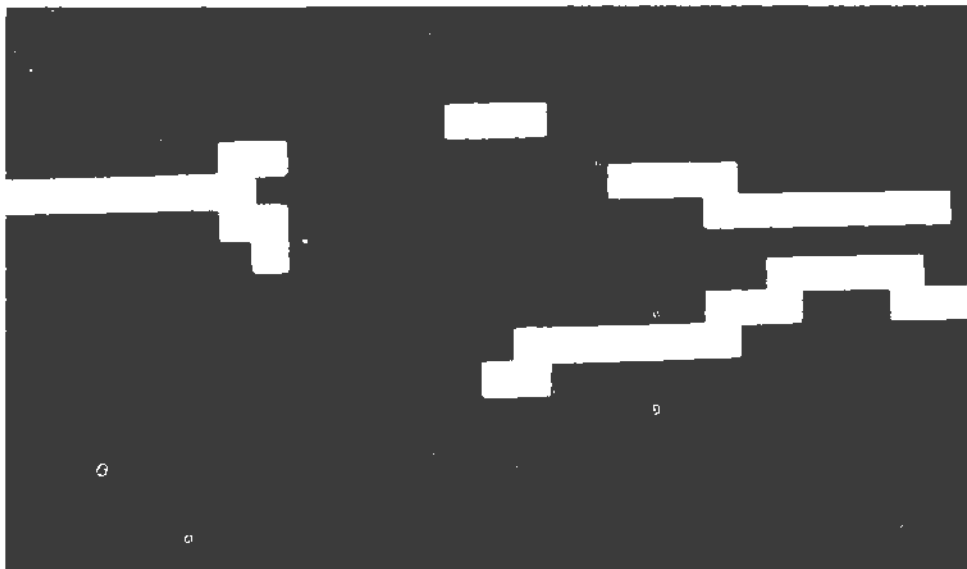


FIG.7

Fig.7. *Close-up on typical crack line structure in the final binary image.*

5. THE RESULTS.

In order to translate the above two-dimensional results to results related to the three-dimensional crack distribution it is necessary to make some assumptions about the geometry of the crack pattern and to make use of results derived from a science which is devoted exactly to that kind of extrapolation: stereology.

Here we assume, that the crack surface can be divided into two classes, one which contains cracks oriented normal to the y- direction and one which contains randomly distributed cracks.

First the absolute crack lengths are converted to specific crack lengths L_x, L_y :

$$L_x = \ell_x/A, \quad L_y = \ell_y/A$$

where A is the total image area.

Now, it follows directly from the assumptions made above and the results from /6/, that

$$\begin{aligned} S_v &= L_x + L_y \\ \Omega &= \frac{L_x - L_y}{L_x + L_y} \\ n &= L_x \end{aligned}$$

where S_v is the total specific crack surface (area per volume), Ω is a convenient measure for orientation varying between 1 (aligned cracks) and 0 (randomized cracks), and n is the specific number of crack/ fiber intersections (per length of the fiber).

Results for the development of S_v and Ω as function of axial strain is shown in fig.8 for the same specimens referred to in fig.2.

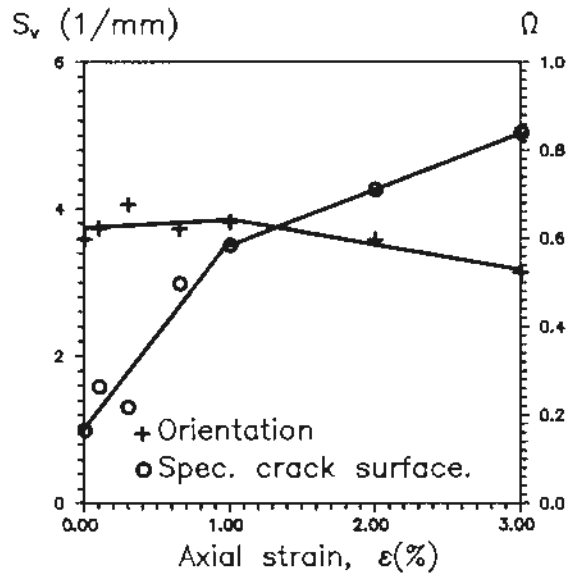


FIG. 8

Fig.8. Development of S_v and Ω as functions of axial strain for the specimens referred to in fig. 2.

6. PRACTICAL ASPECTS

The relationship between specific crack surface and axial strain can be characterized in the following way: At zero strain a specific crack surface of about 1 mm^{-1} is detected. Furthermore, the relationship can roughly be divided into two parts: a steep part for strains between zero and 1% and a much flatter part between 1% and 3% strain. With respect to the relation between the orientation measure and the axial strain it seems as if this two part description applies to that relation as well: from zero to 1% strain the orientation measure is almost constant while a negative slope is observed from 1% to 3% strain.

These observations can be interpreted in the following way: initial cracking caused by non-mechanical loading is observed. This initial cracking is probably caused by early shrinkage in the mould. The specimens are constrained in the axial direction in the mould (see /4/) which could explain the unidirectional character of the initial cracks, see fig.8.

The steep portion of the specific crack surface/ axial strain relationship is related to the formation of multiple cracks. It follows that straining of the specimens is accomplished by formation of cracks rather than opening of a few (localization). The crack formation process continues until 1% strain is reached. This strain level is often referred to as the saturation

level. After this level has been reached the rate of crack formation is much lower indicating that strain is now accomplished by a combination of crack opening and formation. The accompanying drop in the orientation measure might simply reflect that the tortuosity of the cracks is more easily detected on cracks that have opened more than a pixel width.

The determination of the crack saturation level is important in FRC applications where the crack opening is critical e.g. where water penetration and durability aspects need to be carefully controlled.

Furthermore, the analysis described can provide the quantitative data needed in order to calibrate theoretical models for FRC material behaviour as shown in /7/.

Finally, the possibility of applying digital image analysis in the calibration of accelerated durability tests by providing quantitative measures for the material degradation should be mentioned.

7. DISCUSSION

Even though the procedure described above is automatic and in that sense unbiased it is important to note that a number of choices are made - implicitly or explicitly - during the procedure which affects the results.

First of all the choice of equipment, i.e. the magnification of the microscope, the light intensity in the microscope, the resolution and characteristics of the video camera, and the resolution of the digital image - all these factors influence the results obtained by the method.

Secondly the segmentation level i is chosen according to the criterion 'that all significant crack pixels are included'. This is clearly not an objective criterion and it should be noted that the segmentation level does influence the results obtained.

There is really no way of describing how to determine all these parameters, thus the system can only be calibrated using a visual inspection comparing the cleaned binary crack image (fig. 6) with observations in the microscope. However, once the system parameters are determined it is of vital importance to keep the parameters constant in a complete test series. Especially it is important to keep the magnification and the image resolution, i.e. the pixel size, and the segmentation level constant. It really makes no sense to report measurements of crack density without at the same time reporting the pixel size used in the measurements.

The pixel size used in the present investigation was $4.5 \mu\text{m}$ thus the present analysis is not able to detect cracks with a crack opening less than about $2 \mu\text{m}$. However, it is believed that this is sufficiently small in order to ensure that the cracks which are significant with respect to the mechanical behavior of the specimens are detected. This has recently been shown theoretically in /7/.

8. ACKNOWLEDGEMENTS

The digital image analysis and processing described here was carried out on a TN8502 image analysis system at Department of Civil Engineering, Northwestern University.

I wish to thank Professor S.P. Shah and Dr. Barzin Mobasher, both at Northwestern University, for their corporation and valuable assistance with the image analysis work.

I also gratefully acknowledge the support from the Danish Council for Scientific and Industrial Research (Grant Number 16-4239.B) and from "Grosserer Emil Hjort og Hustrus Legat", which made my stay at Northwestern University possible.

9. REFERENCES

- /1/ Castleman, K.R. *Digital Image Processing*, Prentice-Hall, 1979.
- /2/ Rosenfield, A. and Kak, A.C. *Digital Picture Processing*, Academic Press, 1982.
- /3/ Nieblack, W. *An Introduction to Digital Image Processing*, Prentice-Hall, 1986.
- /4/ Krenchel, H. and Stang, H. Stable Microcracking in Cementitious Materials. In *Brittle Matrix Composites 2*. (Eds. A.M. Brandt and I.H. Marshall). Elsevier Applied Science, 1989 pp. 20-33.
- /5/ Stang, H. Stable Microcracking of FRC-materials, *Nordisk Betong* p.49 no.3-4 1987.
- /6/ Underwood, E.E. *Quantitative Stereology*, Addison-Wesley Publishing Company, 1970.
- /7/ Stang, H. and Shah, S.P. Damage Evolution in FRC Materials. Modelling and Experimental Observations. In *Fibre Reinforced Cements and Concretes. Recent Developments*. Eds. R.N. Swamy and B. Barr. Elsevier Applied Science, 1989 pp. 378-387.